

# Electron density and plasma waves in mid-latitude sporadic- $E$ layer observed during the SEEK-2 campaign

M. Wakabayashi<sup>1</sup>, T. Ono<sup>1</sup>, H. Mori<sup>2</sup>, and P. A. Bernhardt<sup>3</sup>

<sup>1</sup>Graduate School of Science, Tohoku University, Sendai, Miyagi, Japan

<sup>2</sup>National Institute of Information and Communications Technology, Tokyo, Japan

<sup>3</sup>Naval Research Laboratory, Washington, DC, USA

Received: 15 December 2004 – Revised: 19 August 2005 – Accepted: 16 September 2005 – Published: 13 October 2005

Part of Special Issue “SEEK-2 (Sporadic- $E$  Experiment over Kyushu 2)”

**Abstract.** The SEEK-2 campaign was carried out over Kyushu Island in Japan on 3 August 2002, by using the two sounding rockets of S310-31 and S310-32. This campaign was planned to elucidate generation mechanisms of Quasi-Periodic Echoes (QPEs) associated with mid-latitude sporadic- $E$  ( $E_s$ ) layers. Electron number densities were successfully measured in the  $E_s$  layers by using the impedance probe on board two rockets. The plasma waves in the VLF and ELF ranges were also observed on board the S310-32 rocket. Results of electron density measurement showed that there were one or two major peaks in the  $E_s$  layers along the rockets' trajectories near the altitude of about 100 km. There were some smaller peaks associated with the main  $E_s$  layers in the altitude range from 90 to 120 km. These density peaks were distributed in a very large extent during the SEEK-2 campaign. The  $E_s$  layer structure is also measured by using the Fixed Bias Probe (FBP), which has a high spatial resolution of several meters (the impedance probe has an altitude resolution of about 400 m). The comparison with the total electron content (TEC) measured by the Dual Band Beacon revealed that the  $E_s$  layer was also modulated in the horizontal direction with the scale size of 30–40 km. It was shown that the QP echoes observed by the ground-based coherent radar come from the major density peak of the  $E_s$  layer. The plasma wave instrument detected the enhancement of VLF and ELF plasma waves associated with the operation of the TMA release, and also with the passage of the  $E_s$  layers.

**Keywords.** Ionosphere (Ionospheric irregularities; Mid-latitude ionosphere; Plasma temperature and density)

## 1 Introduction

Since the first discovery in the 1930's, mid-latitude sporadic- $E$  ( $E_s$ ) layers have been often studied, based on the observations by ionosondes, incoherent scatter radars (ISR), and sounding rockets. There were also many theoretical works, as reviewed by Whitehead (1970, 1989) and Mathews (1998).

The generation mechanism of the mid-latitude  $E_s$  layer is described in terms of the vertical transportation mechanism, due to the neutral wind shear, which creates an enhanced ionization layer. This mechanism was first suggested by Dungey (1958) and extended by Whitehead (1961) and Axford (1966). Wind shear theory has been widely accepted because the measured altitude of the  $E_s$  layer agrees well with the results of the neutral wind measurement (e.g. Sodium or Tri-Methyl-Aluminum (TMA) release experiment). However, several investigations showed the possibility that the  $E_s$  layer is not only contributed by the neutral wind (as “classical” wind shear theory), but also by the ionospheric electric field (Rees et al., 1976).

The basic understanding of the  $E_s$  layer has been verified by many observations using rockets and radars. The mid-latitude  $E_s$  layer has been characterized by its appearance at the altitude of about 100 km with a thickness of 1–3 km, and distributed in the large horizontal extent over several hundreds km (e.g. Oya, 1967; Smith and Mechtyly, 1972). Oya (1967) reported fine structure of  $E_s$  layers and suggested that the  $E_s$  vertical fine structure with altitude intervals of several km.

The  $E_s$  layers have often been observed as multiple peak structures with altitude intervals of several-10 km by using sounding rockets (e.g. Bowen et al., 1964; Smith, 1966; Kato et al., 1972). Smith and Miller (1980) reported the double peaked  $E_s$  layer in the adjacent altitude. These observations were mainly aimed at evaluating the wind shear theory;

however, some examples were not correspondent with wind shear altitude (Bowen et al., 1964).

On the other hand, rocket observations are restricted to measurements of in-situ plasma density along the trajectories. Thus, the horizontal structure of the  $E_s$  layers has also been questioned (e.g. Miller and Smith, 1975) if it is horizontally uniform nature or in a patchy plasma cloud structure. The wind shear theory gives a good description of the measured vertical structure of  $E_s$ , however, this theory cannot give a satisfactory description of the problems with respect to the horizontal extent and the seasonal variation of the occurrence probability, which has a maximum in summer. In addition, mid-latitude  $E_s$  layers have been found to be associated with the various phenomena in the  $E$  region. The intermediate layer (or Tidal Ion Layer, (Fujitaka and Tohmatsu, 1973)) and Ion Rain (e.g. Mathews et al., 1997) were mainly observed by using the ISR located at the Arecibo observatory (18.3°N, 66.75°W). On the other hand, the Quasi-Periodic Echoes (QPEs), having the period of about 5-10 min and their echo trends which seem to move downward with a quasi-periodic motion, were first identified by the MU (Middle and Upper atmosphere) radar observation (Yamamoto et al., 1991) (the MU radar is located at 34.9°N, 136.1°E). It has been revealed that the QPEs often appear to be associated with the occurrence of the  $E_s$  layer, particularly in the nighttime sector in the summer season. The generation mechanism of the QPEs has not yet been clarified, although there have been many discussions among workers. Two models were proposed by Woodman et al. (1991) and Tsunoda et al. (1994). They were based on the vertical modulation of the  $E_s$  layer due to atmospheric gravity waves. The former model assumes several  $E_s$  layers which are separated in altitude, and are modulated as a wave-like form due to gravity waves. Due to the high mobility of the plasma along the magnetic field, the modulated structure of the  $E_s$  layer tends to be aligned along the direction of magnetic field line. Consequently, the field-aligned irregularity (FAI) will be developed along the magnetic field, and it is possible to reflect the radar signal which creates the QPEs. The latter model consists of a single  $E_s$  layer whose altitude is largely modulated as a waveform with an amplitude of  $\pm 15$  km.

To evaluate these models, a comprehensive observational campaign was needed, including direct measurements of the ionosphere during the QP phenomena measured from the ground. The SEEK (Sporadic-*E* Experiment over Kyushu) campaign was carried out in August, 1996, to realize this study. In this campaign, comprehensive observations were made using two sounding rockets successively launched, and ground-based instruments of the VHF radar and optical cameras (Fukao et al., 1998). Two rockets were launched with an interval of 5 days, and many important observational results have been obtained from the campaign. The  $E_s$  layers were detected at almost the same altitude of about 100 km (Yamamoto et al., 1998), which is consistent with the wind shear model predicting an accumulation layer of ions. Additional enhancements of plasma density were also observed at higher altitudes of 110 km, above the main  $E_s$  layer. Strong

electric fields about 10 mV/m were also observed, associated with the  $E_s$  layers.

After the SEEK campaign, the alternative models of the QPEs are proposed by several workers. Yamamoto et al. (1998) proposed a new model, and suggested that two  $E_s$  layers at an altitude of about 100 km and 110 km probably caused FAI. When a disturbance region drifts by  $\mathbf{E} \times \mathbf{B}$  toward the radar site, it may be observed as the QPE phenomena from the ground. Ogawa et al. (2002) pointed out the possibility of the FAI region expanding along the magnetic field line from the dense plasma area that forms the  $E_s$  layer. Ogawa et al. (2002) also showed that the plasma disturbance is drifting toward the southwest, due to  $\mathbf{E} \times \mathbf{B}$ . In all of these models, the  $E_s$  layer plays a significant role in generating the QPEs, and one needs to investigate the detail structure and dynamics of the  $E_s$  layer for further understanding of the QPE phenomena, as well as the  $E_s$  layers.

For the purpose of understanding the structure and dynamics of the mid-latitude  $E_s$  phenomena, the SEEK-2 campaign was carried out on 3 August 2002. On board the two sounding rockets, S310-31 and S310-32, we carried out the measurement of the electron number density by using the impedance probe. Also, plasma wave observation (electric field component) in the  $E_s$  layer was carried out on board S310-32. Based on the results obtained by the SEEK-2 campaign, detailed structure of  $E_s$  layers are examined, as well as other observations, to understand the generation mechanism of the  $E_s$  layer.

## 2 Instrument

To obtain accurate plasma density profiles associated with the nighttime  $E$ -region, we prepared the NEI (Number density of Electrons by Impedance probe) instruments on board the S310-31 and S310-32 sounding rockets for the SEEK-2 campaign. The impedance probe instrument was originally developed by Oya (1966) and installed in various sounding rockets and satellites because of its exclusively high performance for the plasma density measurement in space (e.g. Oya and Obayashi, 1966, Oya et al., 1975, 1990; Yamamoto et al., 1998).

The NEI instrument is able to measure the absolute electron number density by detecting the Upper Hybrid Resonance (UHR) frequency of the ionospheric plasma. The basic equation of the measurement is

$$N_e = 1.24 \times 10^4 \left( f_{\text{UHR}}^2 - f_c^2 \right), \quad (1)$$

where  $N_e$ ,  $f_{\text{UHR}}$  and  $f_c$  are electron number density (/cc), UHR frequency (MHz), and cyclotron frequency (MHz), respectively. The impedance probe also has the advantage that the variation of the probe potential does not affect the measurement.

Detection of the UHR frequency is possible by measuring the frequency dependence of the probe impedance immersed in plasma. When an RF electric field with a swept frequency is applied to the probe, the probe impedance becomes infinite

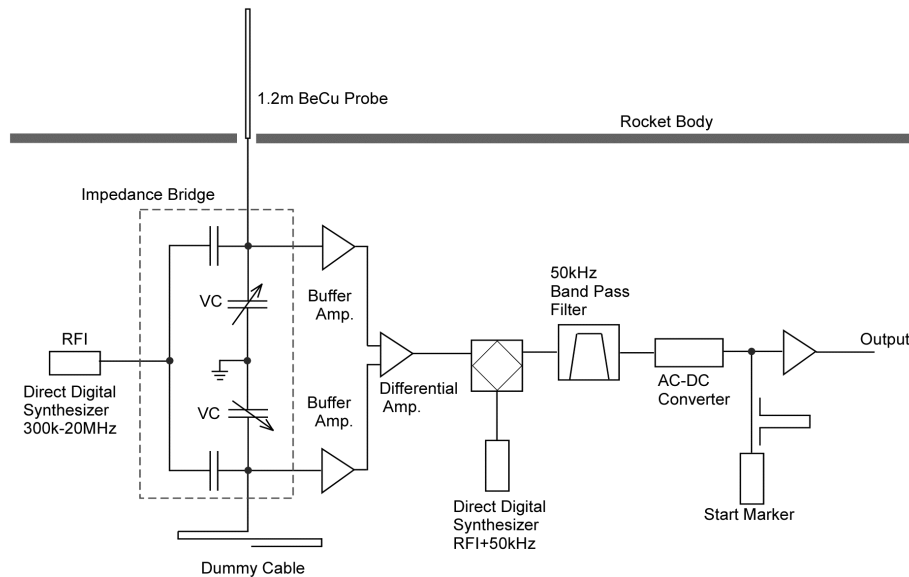


**Fig. 1.** The block diagram of NEI on board the S310-31 and S310-32 rockets. The bridge circuit is enclosed with a dashed line.

when the RF frequency coincides with the UHR frequency. In order to observe the accurate electron number density with this method, it is essential to eliminate any stray capacity in the electrical circuit. For this purpose, an impedance bridge circuit is adopted, as shown in Fig. 1, to cancel out the effect of the stray capacity by adjusting the compensation capacitor and a dummy cable associated with the impedance bridge.

For the SEEK-2 campaign, two improvements had been applied to the NEI instrument. One is the usage of the Direct Digital Synthesizer (DDS) to generate the swept frequency signals, whereas the previous NEI instrument used an analog circuit with the Voltage Controlled Oscillator (VCO) (e.g. Yamamoto et al., 1998). The DDS is able to generate a signal within a frequency range from 300 kHz to 20 MHz, with a step width of 10 kHz (300 kHz–3.8 MHz) and 50 kHz (3.8 MHz–20 MHz), respectively. These step widths are determined to satisfy the requirement of high frequency resolution for the UHR detection. Another improvement was that the impedance bridge circuit with the differential amplifier, which made it possible to install the probe of the instrument near the top of the rocket body, to reduce the effect of the rocket wake.

The accuracy of electron density measurement using NEI depends on the cancellation technique of the stray capacity in the electric circuit itself. This cancellation is achieved by the accurate adjustment of the bridge circuit, to realize the observation accuracy of NEI, less than  $\pm 3\%$  (Oya et al., 1966) in the region whose electron number density is over  $10^4/\text{cc}$ .

In the ionospheric *D*-region, the collision effect between electrons and neutrals becomes significant, compared with the electron cyclotron frequency. The collision effect on the observed UHR frequency should be taken into account for the data analysis, as it has been carried out by Yamamoto et al. (1998). The frequency shift of the UHR waves by the

collision effect is described as follows:

$$v_{en} = 6 \times 10^{-9} N_n, \quad (2)$$

$$f_{\text{UHR}}^2 = f_{ob}^2 - v_{en}^2, \quad (3)$$

where  $v_{en}$  and  $N_n$  represents the collision frequency ( $\text{s}^{-1}$ ) between electrons and neutrals, and number density ( $/\text{cc}$ ) of neutral gases in the ionosphere, respectively, which is obtained by the MSIS-E-90 atmosphere model. In Eq. (3),  $f_{\text{UHR}}$  is the UHR frequency of the ambient plasma, and  $f_{ob}$  is the UHR frequency observed by the NEI instrument. In the region above 100 km altitude, this effect becomes negligible where the difference between  $f_{\text{UHR}}$  and  $f_{ob}$  is smaller than 1%, because  $v_{en}$  decreases rapidly with altitude.

On-board the S310-31 rocket, the electron density and its fluctuation were also measured by the Fixed Bias Probe (FBP), to obtain the plasma irregularities in the  $E_s$  layer with a high spatial resolution of about several meters, as used in the SEEK campaign (Mori and Oyama, 1998). The principle of the FBP instrument is the current measurement of a spherical probe located on the top of the rocket immersed in the ambient plasma, with the DC voltage of 5 V being added. The FBP measures both the DC and AC components of the probe current.

In the present SEEK-2 campaign, the PWM (Plasma and Wave Monitor) instrument was used to measure plasma waves in the VLF and ELF ranges which might be generated in the  $E_s$  layer.

The electric circuit of PWM was integrated with that of the NEI for S310-32. The 2.4-m tip-to-tip dipole antenna was used to measure the plasma waves. The antenna element itself was a 1.2-m ribbon antenna which is identical to the electrode of the NEI. Figure 2 shows the block diagram of the PWM receiver which is connected to the dipole antenna on the left side. The observed plasma waves are separated

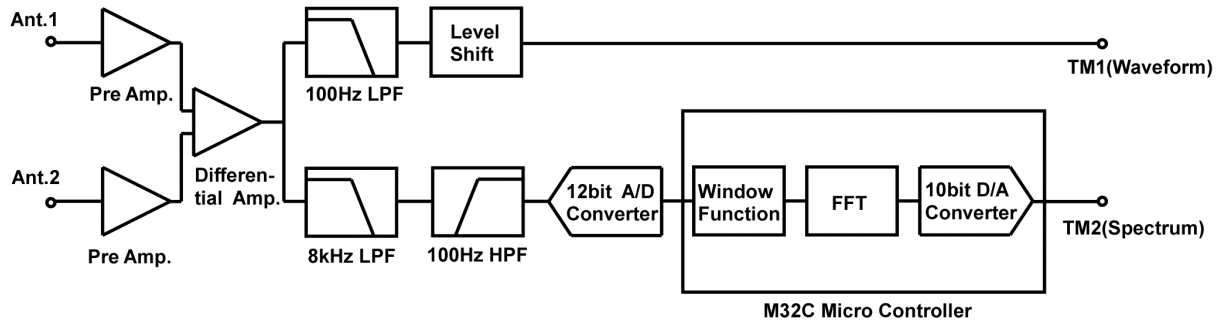


**Fig. 2.** The block diagram of PWM. The left side is the BeCu (Beryllium-Copper) dipole antenna, and the detected wave is subtracted by the differential amp. Output of the upper side is raw data (lower frequency); on the other hand, on the lower side is spectrum data (higher frequency).

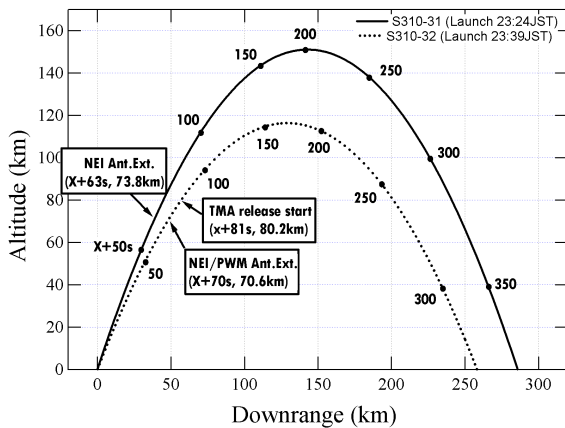


**Fig. 3.** Rocket trajectories traced by 5.6 GHz radar transponders. NEI and PWM observations were carried out above the altitude of 73.8 km (S310-31, NEI) and 70.6 km (S310-32, NEI/PWM), respectively. The TMA release experiment started at the altitude of 80.2 km.

into 10–100 Hz and 100 Hz–10 kHz bands; the former signal is transferred to the telemetry system as waveform data, while the latter is analyzed with an onboard CPU applying FFT (Fast Fourier Transform). The signals are identified as PWM1 (waveform) for the former and PWM2 (spectrum) for the latter. The threshold level of the plasma wave detection is set to  $-110$  dBV ( $3.1 \mu\text{V}_{rms}$ ) with the dynamic range of more than 60 dB. By using the 2.4-m tip-to-tip dipole antenna, the electric field component of the plasma waves are detected with the sensitivity of  $2.5 \mu\text{V/m}$ . TMA release was aimed to measure the neutral wind and continued during the PWM experiment. The TMA release was controlled by a solenoid valve with 1 s ON/1 s OFF (or 2 s ON/4 s OFF) intervals.

### 3 Observation results

#### 3.1 SEEK-2 campaign

The SEEK-2 campaign was planned with two rocket experiments to be launched successively from the Uchinoura Space Center within intervals of 15 min. Ground-based instruments (VHF and MF radar, ionosonde, and optical cameras) were also prepared for this observation. The rocket experiment was carried out on 3 August 2002 with successive launches of the S310-31 and S310-32 rockets at 23:24 JST and 23:39 JST, respectively. This point is one of the main advantages in comparison with the SEEK campaign in 1996. Almost all of the onboard instruments worked perfectly. During the rocket experiments, intense QP echo phenomena appeared.

#### 3.2 Observation geometry and time sequences

As reported by Yamamoto et al. (2005), two rockets were launched at Uchinoura Space Center (USC,  $31.15^\circ$  N,  $13.04^\circ$  E) in the south of Kyushu Island, Japan. Figure 3 shows the rocket trajectories.

After the release of the rocket nosecone, NEI and PWM observations were started 63 s after launch for S310-31 and 70 s after launch for S310-32, respectively. The FBP observation was started at 60 s after launch. NEI and PWM observations were performed above the altitude of 73.8 km for the S310-31 and 70.6 km for S310-32. The maximum altitudes of the S310-31 and S310-32 rockets were about 151 km and 116 km, respectively.

#### 3.3 NEI observation results

Figures 4a and b show measured electron number density profiles on board S310-31 and S310-32, respectively. We collected the collision effects between electrons and neutral particles below 100 km altitude, based on the MSIS-E-90 atmospheric model. As described in Sect. 2, the observation error should be taken into account in the lower density region: Expected errors are plotted by error bars in Figs. 4a

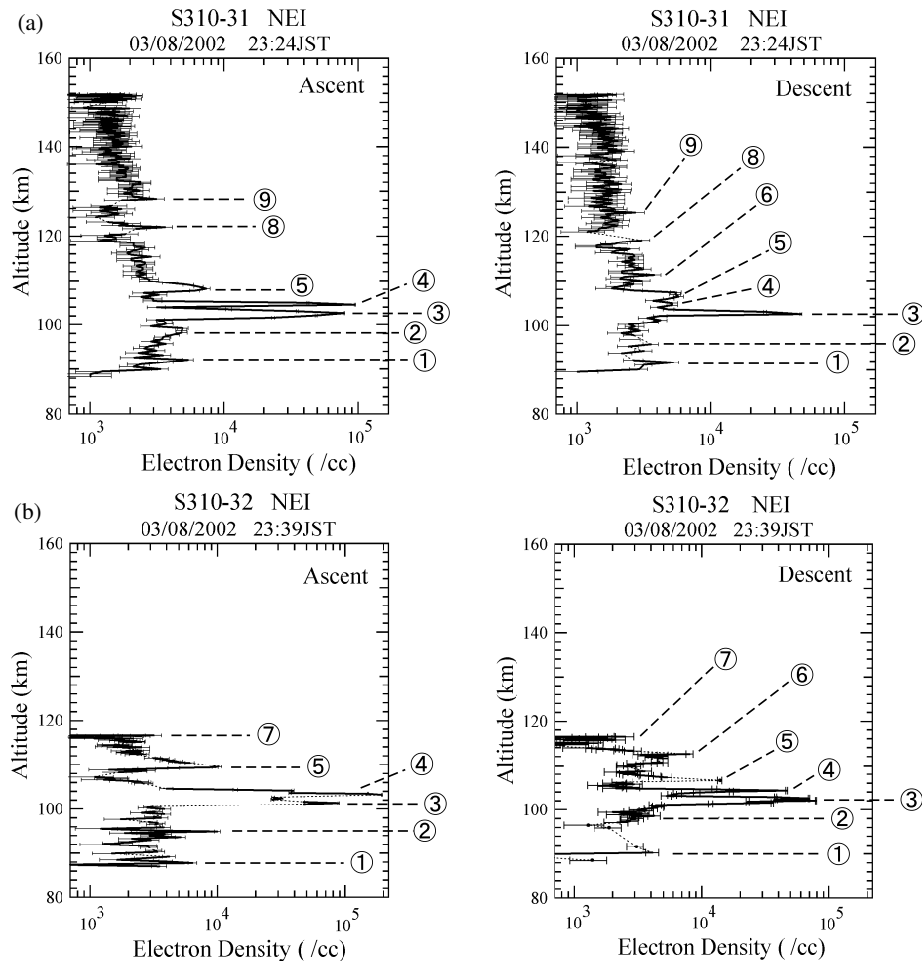


**Fig. 4.** (a) Altitude profiles of electron number density obtained by NEI on board the S310-31 rocket. Error bars show the accuracy of measurement and data interpretation using NEI. There are sharp peaks due to sporadic-*E* layer at the altitude of about 102–105 km. There is only one sharp peak in the descending phase, although there are two sharp peaks in the ascending phase. The peaks in the near altitudes are numbered as the same peaks for the following analysis. (b) Altitude profiles of electron number density obtained by NEI on board the S310-32 rocket. Dashed lines indicate the data blank due to the TMA release.

and b to distinguish meaningful peaks. There are one or two significant peaks of  $E_s$  layers at the altitude of about 100 km. For example, in the ascending phase of S310-31, two very sharp peaks with  $7.9 \times 10^4$  /cc and  $9.5 \times 10^4$  /cc are detected at altitudes of 102.7 km and 104.6 km, respectively. There are also several weak peaks detected in the altitude range between 90 km and 120 km (dashed lines indicate the data blank). The weak peaks are located at altitudes of 92.1 km, 99.2 km, 108.1 km, 122.0 km, and 128.3 km in the ascending phase of S310-31. Hereinafter, the apparent sharp peaks will be called “main peaks”, and the relatively weak peaks will be called “sub peaks”. Within the descending phase of the S310-31 observation, only one main peak was observable. But characteristics of the  $E_s$  layer of the present experiment, including the two main peaks, seems to be common among these profiles. We can identify the existence of several density peaks associated with the  $E_s$  layers throughout the present SEEK-2 rocket observation numbered from

1 to 9, as shown in Fig. 4. The same number means that they appear in the similar altitude range in the ionosphere. These peaks are summarized in Table 1 which also includes the results from the S310-32 rocket. In Table 1, the peaks numbered 3 and 4 are the major density peaks which give the main structure of the  $E_s$  layers. They are detected at a very stable altitude within the altitude range of 2 km for both S310-31 and S310-32 observations. However, the sub-peaks below the main  $E_s$  layer appeared within the altitude range of  $\sim 5$  km. Altitudes of the sub-peaks above the main  $E_s$  seem unstable, depending on the observation chance. It should be noted that the altitude profiles of the  $E_s$  layers, as well as several sub-peaks, show similarity, although there are large horizontal distances over 100 km between the up-leg and downleg of each rocket. In addition, two rockets are launched at intervals of 15 min. This fact suggests that there is a horizontally expanded and stable  $E_s$  region during the rocket experiments. These main features of  $E_s$  are very

**Table 1.** Summary of the peak density location in the altitude profile obtained during the SEEK-2 campaign. The contents of the table represent “peak altitude (km)/peak density (/cc)”. And No. (3) and (4) are the main peaks due to the sporadic-*E* layer.

Peak No.	31 Ascent	31 Descent	32 Ascent	32 Descent
(9)	128.3/3.12e+3	125.3/2.75e+3		
(8)	122.0/3.62e+3	119.1/3.06e+3		
(7)			116.6/3.18e+3	116.4/2.49e+3
(6)		111.3/3.79e+3		112.6/8.02e+3
(5)	108.1/7.33e+3	106.4/5.79e+3	109.6/1.02e+4	106.6/1.39e+4
(4)-main	104.6/9.45e+4	105.0/5.19e+3	103.2/1.92e+5	104.3/4.60e+4
(3)-main	102.7/7.85e+4	102.6/4.74e+4	101.4/8.80e+4	102.1/7.85e+4
(2)	99.2/4.97e+3	95.8/3.40e+3	95.0/1.00e+4	98.6/4.10e+3
(1)	92.1/5.30e+3	91.7/6.47e+3	87.8/6.40e+3	90.3/4.05e+3

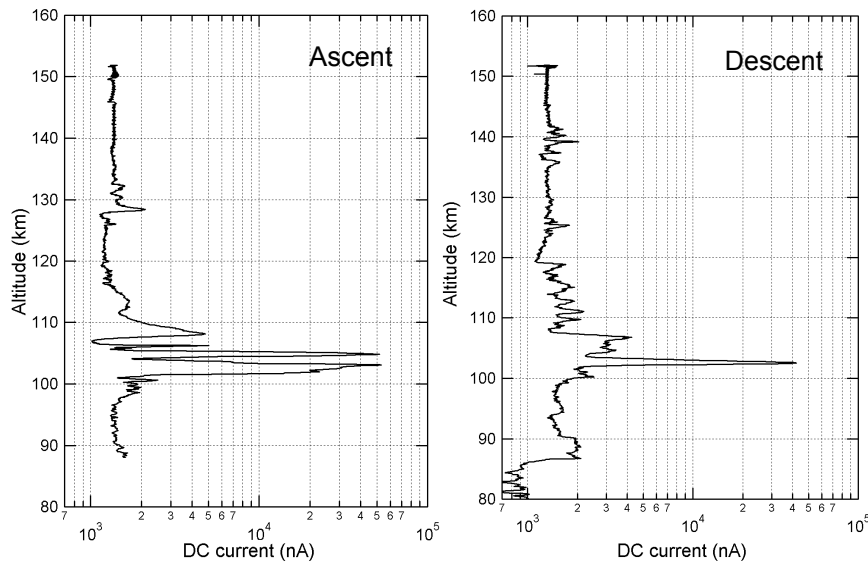


**Fig. 5.** The FBP observation results obtained by the S310-31 rocket. These panels represent DC current components.

similar to the previous results from the SEEK campaign in 1996. The detailed analysis and comparison with previous observations will be described in Sect. 4.

### 3.4 FBP observation results

Results from the FBP experiment are shown in Fig. 5, giving DC currents obtained during the ascending and descending phases of S310-31.

In Fig. 5, DC current profiles correspond with the electron density profiles obtained by NEI. The observed multi-layer structures are reproduced well by the FBP instrument. However, we can find differences between the FBP and NEI at the altitude 122 km in the ascending period. The DC current observed by the FBP instrument is determined not only by the electron density but also by the electron temperature and the probe potential. FBP data at 122 km are possibly affected by

the large fluctuation of electron temperature, as suggested by Oyama et al. (private communication, 2005). On the other hand, FBP results show small current peaks at the altitude of 139 km in the descending phase. This enhancement is also detected by the NEI instrument, although it is too weak to be seen in the error bars. It is noted, due to the discrete sampling of the NEI which has a time resolution of about 500 ms, that there can be seen small differences with the profiles obtained by the FBP experiment. However, as it was found in the identification of the main  $E_S$  layer, the characteristics of the  $E_S$  layer obtained by using the NEI and the FBP experiments are almost the same.

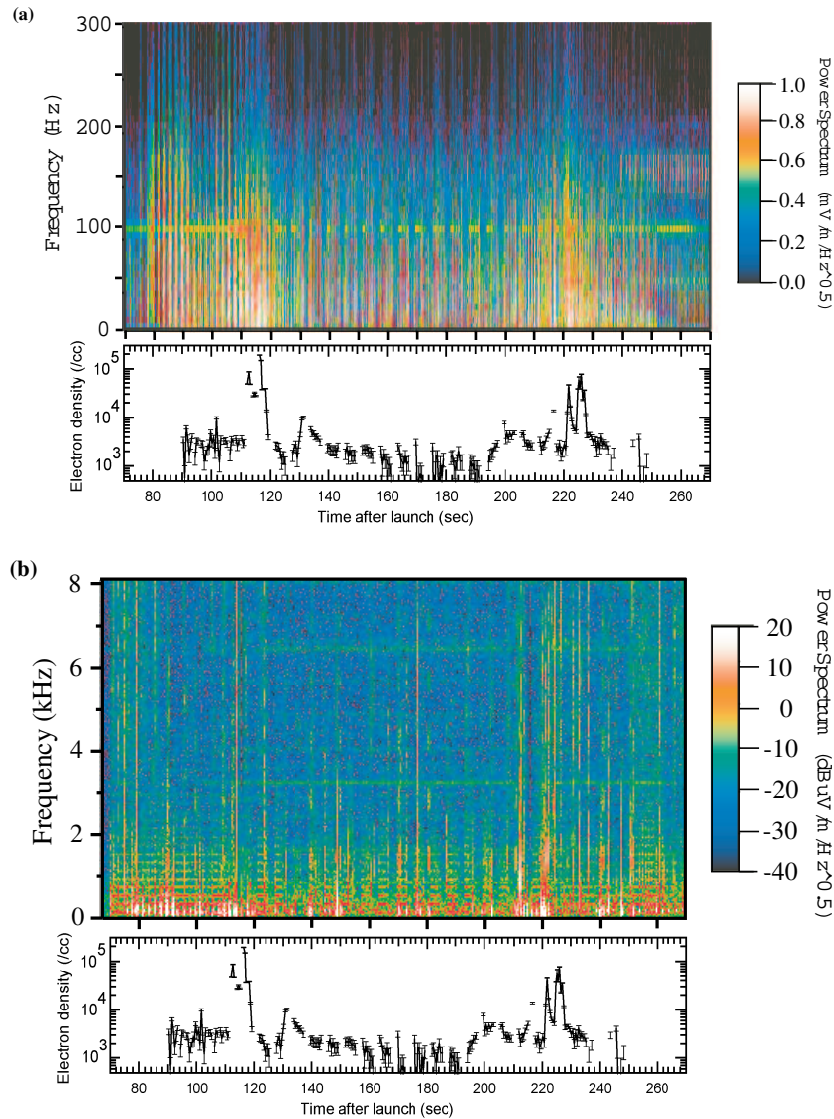


**Fig. 6.** (a) Dynamic spectrum of PWM1 (lower frequency) and its correspondence to the  $E_s$  layer structure. (b) Same figures of PWM2 (higher frequency) as in Fig. 6a.

### 3.5 The dynamic spectrum of the low frequency plasma waves

The dynamic spectra obtained by PWM on board the S310-32 rocket are shown in Figs. 6a (lower frequency range) and b (higher frequency range), respectively. The simultaneous observation data of the electron density is also plotted in the bottom panel. After the antenna extension at 70 s, after the launch, various types of plasma waves were detected by the PWM instrument. The observation was continued until the telemetry lock off at 280 s. As shown in Figs. 6a and b, bursty signatures of plasma waves appeared at synchronized timing with the TMA release. The interval of the TMA release was 1 s ON/1 s OFF, or 2 s ON/4 s OFF depending on the flight time. On the other hand, we can also find the strong wave enhancements associated with the passage of the main  $E_s$

peak, in both ascending and descending phases.

#### 3.5.1 FFT analysis and interpretation of PWM data

After eliminating instrumental interference noise to the PWM1, FFT analysis was applied to 65536 data points with the Humming window. Because the time resolution of PWM1 is 0.3125 ms, the frequency resolution  $\Delta f$  is calculated by the equation of

$$\Delta f = \frac{1}{\Delta t \cdot N} = 0.049 \text{ Hz}, \quad (4)$$

where  $\Delta t$  and  $N$  are the time resolution and the number of data points, respectively. Six panels in Figure 7 show the results of the FFT analysis in the altitude range from 80.0 km to 116.6 km after launch.

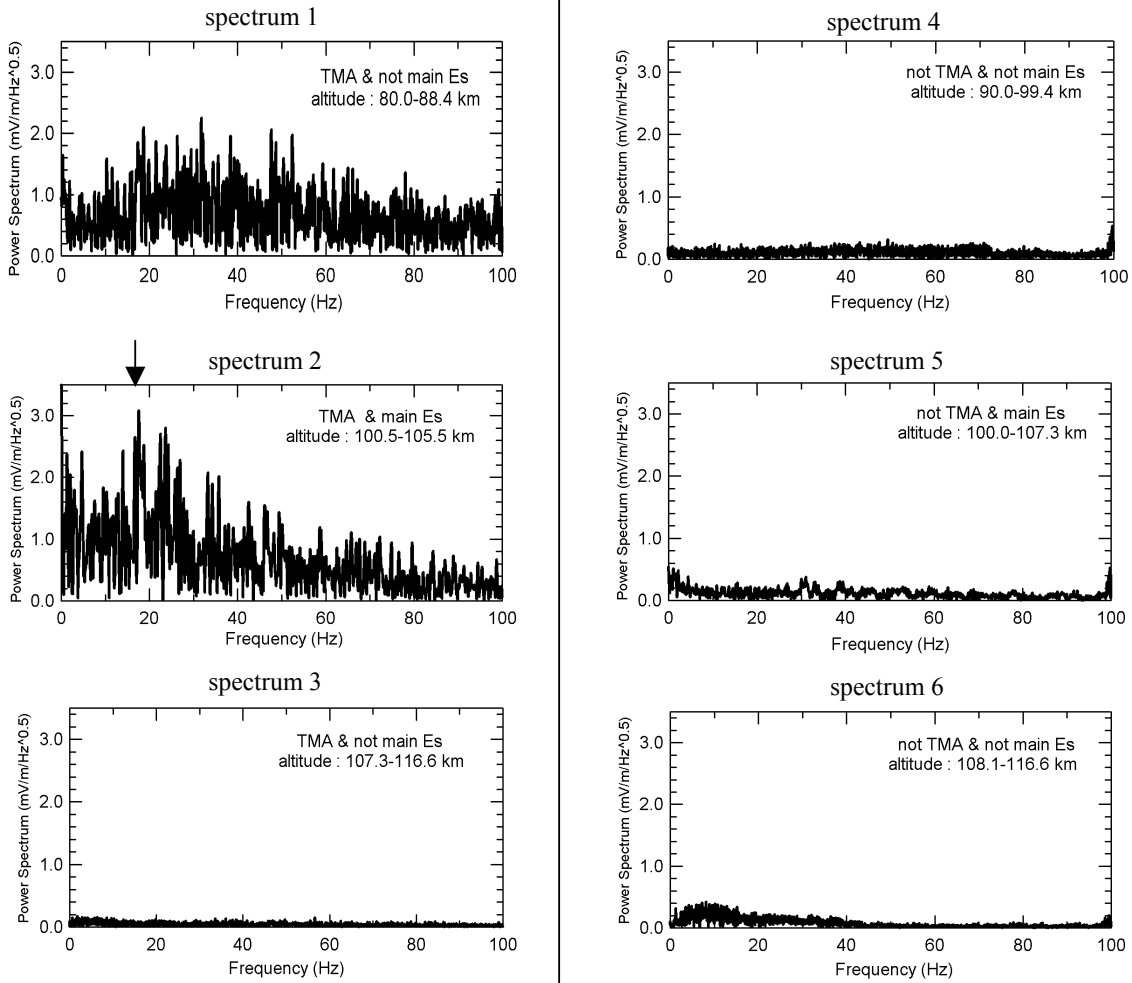


**Fig. 7.** The plasma wave spectrum obtained by using PWM1 (ascending phase). Left (spectra 1–3) and right (spectra 4–6) panels represent the spectrum of TMA ON and OFF in each altitude range, respectively. Characteristic peak at 17.6 Hz is represented by arrow. All enhanced waves are due to the TMA ON. The waves were weakened above the main  $E_s$  layer, even in the TMA ON period.

In Figs. 6a and b, intense plasma waves associated with the passage through the  $E_s$  layers as well as the TMA release operation, are detected. Moreover, when the rocket passed through the  $E_s$  layers, these plasma waves are further intensified. In Fig. 7, the left and right side spectra represent TMA ON and OFF, respectively. These spectra suggest that all the enhanced waves have been associated with the TMA ON either main  $E_s$  layer passage. For example, a comparison of the spectra 1 and 2 shows the difference due to the existence of the main  $E_s$  layer. After the passage of the  $E_s$  layer, the enhancement became a weak signature in the TMA ON. Within the descending time period of the rocket experiment, there is almost the same tendency with respect to the TMA operation, as well as the effect of the  $E_s$  layer.

If plasma waves are generated due to the possible electro-dynamics of the  $E_s$  layer, the detection of the similar spectra is likely to be expected for both the ascending and descending phases. Indeed, there were common spectral peaks near 18–20 Hz. Plasma waves in the frequency range 18–20 Hz are analyzed in more detail using 2048 point FFT. As

a result, the enhancement of the plasma waves near the frequency of 18–20 Hz was also synchronized with the TMA release at around 115–116 s. Then, it can be concluded that these plasma waves are also intensified due to the reaction of the TMA material in the  $E_s$  layer. In particular, these plasma waves are detected at both altitudes of 102.7–103.7 km and 103.7–104.8 km. When we compare plasma waves with the plasma density profiles given in Figs. 4a and b, the present enhancement of the plasma waves appeared to be within a range from the depression region of the electron number density to the upper layer of the  $E_s$ . Considering the frequency and spectral shapes of the plasma waves, the propagation mode is likely to be the ion cyclotron wave. The 18–20 Hz frequencies are well associated with the cyclotron frequency of  $O_2^+$ ,  $Si^+$ , or  $Fe^+$  ions. However, present plasma wave observations are performed in the collision dominant region, where the collision frequency  $\nu_{in}$  reaches up to  $10^2$  Hz. Because the Larmor radii of the ions are several meters, these heavy ions have difficulty to create a complete circular gyro motion in this condition.

#### 4 Discussion

Altitude profiles of the  $E_s$  electron number density obtained during the SEEK-2 campaign revealed the appearance of  $E_s$  peak structures at almost the same altitude. Although there are horizontal distances of about 100 km between the ascending and descending phases of each rocket, the structure of the main  $E_s$  peaks seem to be expanded horizontally over the observation region. This feature is similar to the previous rocket observations (e.g. Smith, 1966). It can be understood that an  $E_s$  layer has a multi-layer structure with two peaks and is associated with several sub-peaks. Smith (1966) mentioned the double-peaked  $E_s$  layer with a steep gradient of density (in other words, a sharp “valley”) which had similar features to the results from the present experiment. By the present experiment, the  $E_s$  layers were confirmed to be accompanied by FAI (Saito et al., 2005). The present SEEK-2 results showed that the many peaks (at most 9 peaks), including the sharp density gradient, are successively detected and existed for at least 15 min during this campaign. This is one of the most significant achievements of the present experiment.

In addition, we compare the results with those from the Dual Band Beacon experiment (Bernhardt et al., 2005), to estimate the horizontal extent of the  $E_s$  layer. In the electron density profiles obtained by the NEI on board the S310-31, there are two sharp peaks in the ascending phase, although there is only one peak in the descending phase. This difference seems to be originated by the horizontal plasma inhomogeneity in the sporadic- $E$  layer. The DBB observation is to survey the horizontal distribution of the electron density by the measurement of Total Electron Content (TEC) value along the path between the rocket and ground-based receiver sites (located on Uchinoura, Tarumizu, and Takasaki). Bernhardt et al. (2005) reported slant TEC values obtained by the S310-31 and S310-32 rockets. The slant TEC value rapidly increased when the rocket passed the  $E_s$  layer and reached the density of  $3\text{--}5 \times 10^{14} \text{ (m}^{-2}\text{)}$ . The TEC value is consistent with the integrated electron density from the NEI measurement (see Figs. 8a and b). Most TEC modulations in the Beacon data describe the electron density modulation in the  $E_s$  layer. The TEC modulation is then projected to the 100 km altitude in Figs. 9a and b. Figure 9a shows the variation in the beacon signal from the DBB on board S310-31, received at Uchinoura. There is some periodic modulation of the TEC values. It is suggested that the  $E_s$  layer plasma was distributed as a plasma cloud or a patchy structure. On the other hand, Fig. 9b shows the data obtained by DBB on board S310-31, received at Tarumizu. There are also modulations of the TEC values due to the distribution of the plasma cloud. As illustrated in Figs. 9a and b, the scale size of the plasma cloud structure is estimated to be between about 20 km and 40 km. In the sporadic- $E$  layer, horizontal plasma irregularities seem to be distributed as plasma clouds, as described above. The difference in peak density detected by the S310-31 (peak number 4) probably reflect such horizontal inhomogeneity of the  $E_s$  layer.

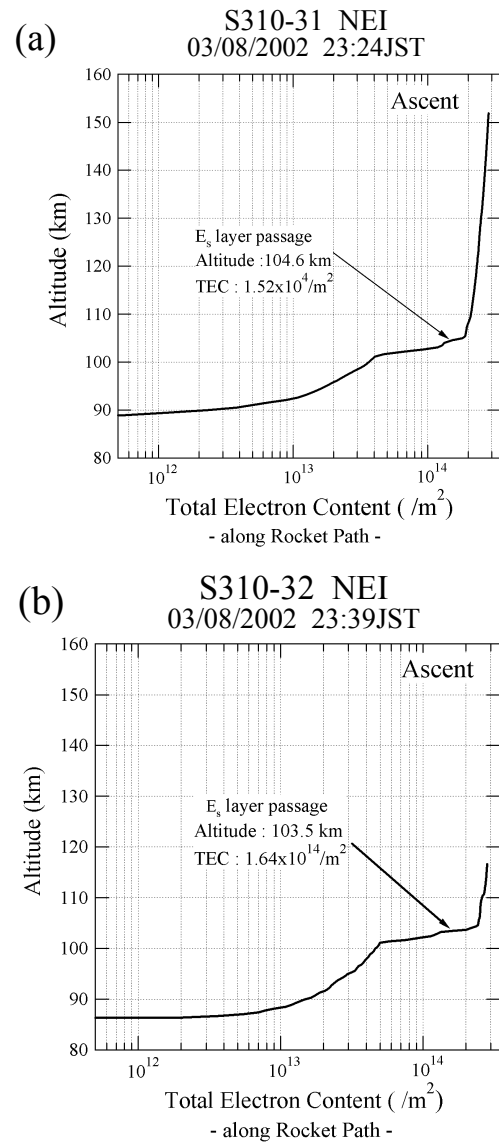


**Fig. 8.** (a) and (b) The integrated values of electron density profiles obtained by the NEI on board S310-31 and S310-32, respectively (integration is performed from the ground in each panel).

In addition, it is suggested that if these plasma structures drifted toward the southwest, the backscatter radar beam would be detected as QP echoes. The DBB experiment on board S310-32 also detected the horizontal modulation of electron density. The scale sizes of plasma clouds were estimated to be a little larger (about 40–50 km) than the case of S310-31 (see, Fig. 10). This difference can be understood by the difference in the observation region (path) because of the time interval of 15 min.

As shown in Sect. 3, intense VLF and ELF plasma waves were identified in the main  $E_s$  layer during the ascending and descending phases of S310-32. The strong plasma waves were detected within the time range from 115.855 s to 117.555 s, which corresponds to the altitude range from 102.7 km to 103.7 km in the ascending phase. In

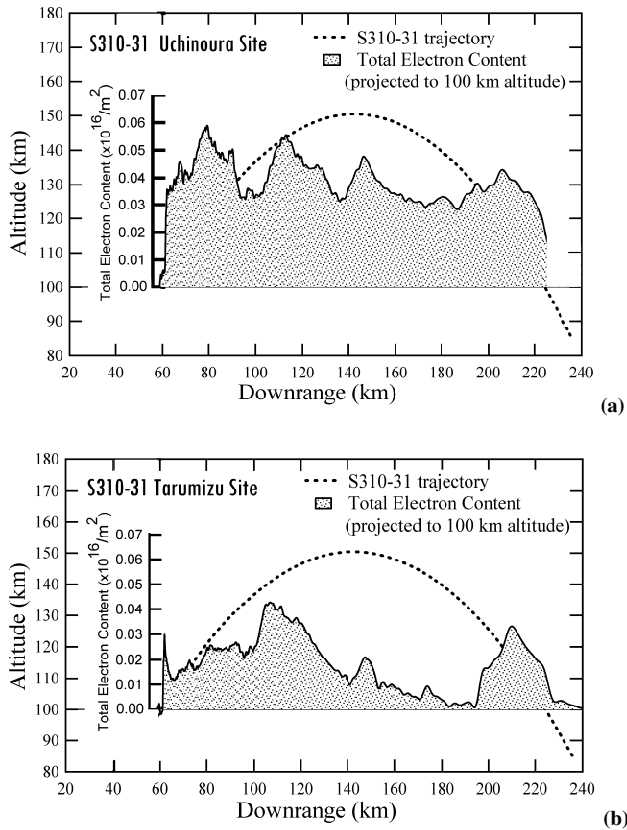


**Fig. 9.** (a) Projection of the TEC values to the 100 km altitude (obtained by the Uchinoura site). Periodical and horizontal modulation of TEC occurs. The scale size of the plasma clouds is estimated to be about 30–40 km. (b) Same as (a) except for the Taramizu site. The scale size of the plasma clouds is estimated to be about 20–50 km.

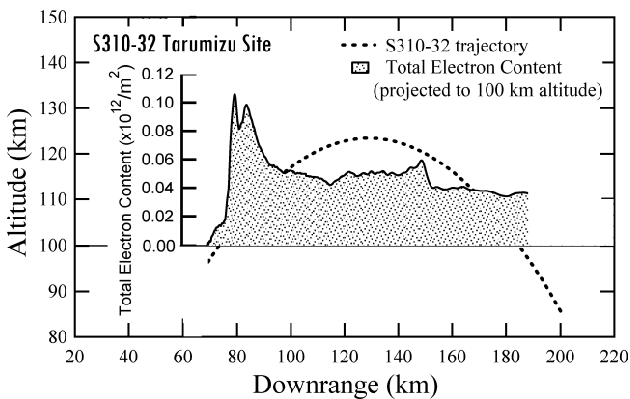


**Fig. 10.** Same as Figs. 9a and b, except for the one obtained by S310-32, received at the Taramizu site. The scale size of the plasma clouds can be estimated to be about 40–50 km, however, its observation region is narrower than S310-31.

the descending phase of the rocket, the strong plasma waves were also observed within the time range from 220.754 s to 223.319 s which corresponds the altitude range from

104.8 km to 103.7 km. These altitude ranges agree well with the upper peak of the observed  $E_s$  in ascending and descending phases. Therefore, these results imply that the upper layer is dominated by an electromagnetic effect in comparison to the lower layer, and it may be generated by the plasma instability associated with the formation of the  $E_s$  ionosphere.

## 5 Conclusions

For the purpose of the study of the QP echo phenomena associated with the  $E_s$  layers, a comprehensive experiment of the SEEK-2 campaign was held by using the S310-31 and S310-32 sounding rockets on 3 August 2002. With the successive launch of the two rockets within intervals of 15 min, the NEI measured the electron density profiles four times without the effect of the rocket wake. The observed  $E_s$  layer had extremely complex height structures. However, they showed common features among the four electron density profiles obtained. These observation results show that there are large horizontal structures with a scale size of more than one hundred km. The structure seems stable, at least within a time period of more than 15 min. The comparison with the total electron content (TEC) measured by the Dual Band Beacon experiment showed that the  $E_s$  layer is also modulated in the horizontal direction with the scale size of 30–40 km. The main  $E_s$  layer consists of horizontal inhomogeneity, as shown by the simultaneous DBB experiment.

In addition, a plasma wave observation was also carried out by the PWM instrument on board S310-32. As the first trial of the plasma wave observation in the  $E_s$  layer, we discovered that the enhancement of the VLF and ELF plasma waves were certainly associated with the  $E_s$  layer. The detailed generation mechanism of these plasma waves is the subject for the future study.

The formation mechanism of the  $E_s$  layer, which shows horizontally broad and vertically complex characteristics, is discussed in a companion paper (Wakabayashi and Ono, 2005). In particular, the double peak density enhancements in the  $E_s$  layers most remarkable characteristics.

*Acknowledgements.* The authors would like to show their thanks to S. Fukao and M. Yamamoto of Kyoto University, M. Iizima and A. Kumamoto of Tohoku University for their important discussions and comments on the present study. The authors also would like to express their thanks to K. Oyama, N. Iwagami, H. Hayakawa, and T. Abe for their cooperation in carrying out the SEEK-2 experiment and for providing the data of the sounding rockets.

The authors wish to express their deep appreciation to the members of System Keisoku Inc. for development of the rocket-borne instruments and to all the members of the ISAS rocket team for the successful achievement of the rocket experiments. Activities of Ono and Wakabayashi are supported by the 21st century COE program “Advanced Science and Technology Center for the Dynamic Earth” at Tohoku University.

Topical Editor M. Pinnock thanks two referees for their help in evaluating this paper.

## References

- Axford, W. I., Cunnold, D. M., and Greeson, L. J.: Magnetic field variations in temperate zone sporadic-*E* layers, *Planet. Space Sci.*, 14, 909–919, 1966.
- Bernhardt, P. A., Selcher, C. A., Siefing, C., Wilkens, M., Compton, C., Bust, G., Yamamoto, M., Fukao, S., Ono, T., Wakabayashi, M., and Mori, H.: Radio tomographic imaging of sporadic-*E* layers during SEEK2, *Ann. Geophys.*, 23, 2357–2368, 2005.
- Bowen, P. J., Norman, K., Willmore, A. P., Baguette, J.-M., Murin, F., and Storey, L. R. O.: Rocket studies of sporadic-*E* ionization and ionospheric winds, *Planet. Space Sci.*, 12, 1173–1177, 1964.
- Dungey, J. W.: *Cosmical Electrodynamics*, 167, Cambridge University Press, 1958.
- Fujitaka, K. and Tohmatsu, T.: A tidal theory of the ionospheric intermediate layer, *J. Atmos. Terr. Phys.*, 35, 425–438, 1973.
- Fukao, S., Yamamoto, M., Tsunoda, R. T., Hayakawa, H., and Mukai, T.: The SEEK (Sporadic-*E* Experiment over Kyushu) campaign, *Geophys. Res. Lett.*, 25, 11, 1761–1764, 1998.
- Kato, S., Aso, T., Horiuchi, T., Nakamura J., and Matsuoka T.: Sporadic-*E* formation by wind shear, comparison between observation and theory, *Radio Sci.*, 7, 359–362, 1972.
- Mathews, J. D., Sulzer, M. P., and Perillat, P.: Aspects of layer electrodynamics inferred from high-resolution ISR observations of the 80–270 km ionosphere, *Geophys. Res. Lett.*, 24, 11, 1411–1414, 1997.
- Mathews, J. D.: Sporadic *E*: current views and recent progress, *J. Atmos. Solar-Terr. Phys.*, 60, 4, 413–435, 1998.
- Miller, K. L. and Smith, L. G.: Horizontal structure of midlatitude sporadic-*E*-layers observed by incoherent scatter radar, *Radio Sci.*, 10, 271–276, 1975.
- Mori, H. and Oyama, K.: Sounding rocket observation of sporadic-*E* layer electron-density irregularities, *Geophys. Res. Lett.*, 25, 11, 1785–1788, 1998.
- Ogawa, T., Takahashi, O., Otsuka, Y., Nozaki, K., Yamamoto, M., and Kita, K.: Simultaneous middle and upper atmosphere radar and ionospheric sounder observations of midlatitude *E* region irregularities and sporadic *E* layer, *J. Geophys. Res.*, 107(A10), 1275, doi:10.1029/2001JA900176, 2002.
- Oya, H.: Study on boundary value problems of magneto-active plasma and their applications to space observation, PhD Thesis, Kyoto University, 1966.
- Oya, H. and Obayashi, T.: Measurement of ionospheric electron density by a gyro-plasma probe: A rocket experiment by a new impedance probe, *Rep. Ionos. Space Res. Japan*, 20, 199–213, 1966.
- Oya, H.: Irregular type sporadic-*E* observed by rocket borne gyro-plasma probe at a temperate latitude, *J. Geomag. Geoelectr.*, 19, 4, 267–272, 1967.
- Oya, H., Morioka, A., and Kondo, M.: Differential precipitation of the low energetic protons and electrons in Brazilian anomaly, Tohoku University, Science Reports, Series 5 – Geophysics, 23, 29–36, 1975.
- Oya, H., Morioka, A., Kobayashi, K., Iizima, M., and Ono, T.: Plasma wave observation and sounder experiments (PWS) using the Akebono (EXOS-D) satellite – Instrumentation and initial results including discovery of the high altitude equatorial plasma turbulence, *J. Geomag. Geoelectr.*, 42, 411–442, 1990.
- Rees, D., Dorling, E. B., Lloyd, K. H., and Low, C.: The role of neutral winds and ionospheric electric field in forming stable sporadic *E*-layers, *Planet. Space Sci.*, 24, 475–478, 1976.
- Saito, S., Yamamoto, M., Fukao, S., Marumoto, M., and Tsunoda, R. T.: Radar observations of field-aligned plasma irregularities in the SEEK-2 campaign, *Ann. Geophys.*, 23, 2307–2318, 2005.
- Smith, L. G.: Rocket observations of sporadic *E* layers and related features of the *E* region, *Radio Sci.*, 1, 178–186, 1966.
- Smith, L.G. and Mechtly, E. A.: Rocket observation of sporadic-*E* layers, *Radio Sci.*, 7, 367–376, 1972.
- Smith, L. G. and Miller, K. L.: Sporadic-*E* layers and unstable wind shears, *J. Atmos. Terr. Phys.*, 42, 45–50, 1980.
- Tsunoda, R. T., Fukao, S., and Yamamoto, M.: On the origin of quasi-periodic radar backscatter from midlatitude sporadic *E*, *Radio Sci.*, 29, 1, 349–365, 1994.
- Wakabayashi, M. and Ono, T.: Multi-layer structure of mid-latitude sporadic-*E* observed during the SEEK-2 campaign, *Ann. Geophys.*, 23, 2347–2355, 2005.
- Whitehead, J. D.: The formation of sporadic-*E* layer in the temperate zones, *J. Atmos. Terr. Phys.* 20, 49–58, 1961.
- Whitehead, J. D.: Production and prediction of sporadic-*E*, *Rev. Geophys. Space Phys.*, 8, 65–144, 1970.
- Whitehead, J. D.: Recent work on mid-latitude and equatorial sporadic-*E*, *J. Atmos. Terr. Phys.*, 51, 5, 401–424, 1989.
- Woodman, R. F., Yamamoto, M., and Fukao, S.: Gravity wave modulation of gradient drift instabilities in mid-latitude sporadic *E* irregularities, *Geophys. Res. Lett.*, 18, 7, 1197–1200, 1991.
- Yamamoto, M., Fukao, S., Woodman, R. F., Ogawa, T., Tsuda, T., and Kato, S.: Midlatitude *E* region field-aligned irregularities observed with the MU radar, *J. Geophys. Res.*, 96, 15 943–15 949, 1991.
- Yamamoto, M., Fukao, S., Tsunoda, R. T., Pfaff, R., and Hayakawa, H.: SEEK-2 (Sporadic-*E* Experiment over Kyushu 2) – Project Outline and Significance, *Ann. Geophys.*, 23, 2295–2305, 2005.
- Yamamoto, M.-Y., Ono, T., Oya, H., Tsunoda, R. T., Larsen, M. F., Fukao, S., and Yamamoto, M.: Structures in sporadic-*E* observed with an impedance probe during the SEEK campaign: Comparisons with neutral-wind and radar-echo observations, *Geophys. Res. Lett.*, 25, 11, 1781–1784, 1998.